


RESEARCH

Open Access



# KCNQ1-deficient and KCNQ1-mutant human embryonic stem cell-derived cardiomyocytes for modeling QT prolongation

Yuanxiu Song<sup>1†</sup>, Tianwei Guo<sup>2†</sup>, Youxu Jiang<sup>6†</sup>, Min Zhu<sup>3</sup>, Hongyue Wang<sup>3</sup>, Wenjing Lu<sup>4</sup>, Mengqi Jiang<sup>5</sup>, Man Qi<sup>3</sup>, Feng Lan<sup>4\*</sup> and Ming Cui<sup>1\*</sup> 

## Abstract

**Background:** The slowly activated delayed rectifier potassium current ( $I_{Ks}$ ) mediated by the KCNQ1 gene is one of the main currents involved in repolarization. *KCNQ1* mutation can result in long-QT syndrome type 1 (LQT1).  $I_{Ks}$  does not participate in repolarization in mice; thus, no good model is currently available for research on the mechanism of and drug screening for LQT1. In this study, we established a *KCNQ1*-deficient human cardiomyocyte (CM) model and performed a series of microelectrode array (MEA) detection experiments on *KCNQ1*-mutant CMs constructed in other studies to explore the pathogenic mechanism of *KCNQ1* deletion and mutation and perform drug screening.

**Method:** *KCNQ1* was knocked out in human embryonic stem cell (hESC) H9 line using the CRISPR/cas9 system. *KCNQ1*-deficient and *KCNQ1*-mutant hESCs were differentiated into CMs through a chemically defined differentiation protocol. Subsequently, high-throughput MEA analysis and drug intervention were performed to determine the electrophysiological characteristics of *KCNQ1*-deficient and *KCNQ1*-mutant CMs.

**Results:** During high-throughput MEA analysis, the electric field potential and action potential durations in *KCNQ1*-deficient CMs were significantly longer than those in wild-type CMs. *KCNQ1*-deficient CMs also showed an irregular rhythm. Furthermore, *KCNQ1*-deficient and *KCNQ1*-mutant CMs showed different responses to different drug treatments, which reflected the differences in their pathogenic mechanisms.

**Conclusion:** We established a human CM model with *KCNQ1* deficiency showing a prolonged QT interval and an irregular heart rhythm. Further, we used various drugs to treat *KCNQ1*-deficient and *KCNQ1*-mutant CMs, and the three models showed different responses to these drugs. These models can be used as important tools for studying the different pathogenic mechanisms of *KCNQ1* mutation and the relationship between the genotype and phenotype of *KCNQ1*, thereby facilitating drug development.

**Keywords:**  $I_{Ks}$ , *KCNQ1*, LQT, hESCs, CRISPR/cas9

## Introduction

Long-QT syndrome (LQTS) is a cardiogenetic disorder that can cause life-threatening arrhythmias and is associated with sudden cardiac death [1, 2]. Long-QT syndrome type 1 (LQT1) is the most prevalent subtype, accounting for approximately 40–50% of all patients with LQTS [3]. Studies have reported that LQT1 is caused by loss-of-function mutations in *KCNQ1* that encodes the  $\alpha$

<sup>†</sup>Yuanxiu Song, Tianwei Guo and Youxu Jiang have contributed equally to this work

\*Correspondence: fenglan@fuwai.com; mingcui@bjmu.edu.cn

<sup>1</sup> Department of Cardiology, Peking University Third Hospital, 49 Huayuan North Road, Haidian District, Beijing 100191, China

<sup>4</sup> Shenzhen Key Laboratory of Cardiovascular Disease, Fuwai Hospital Chinese Academy of Medical Sciences, Chinese Academy of Medical Sciences and Peking Union Medical College, Shenzhen 518057, China Full list of author information is available at the end of the article



subunit of the cardiac Kv7.1 potassium channel mediating the slowly activated delayed rectifier potassium current ( $I_{Ks}$ ) [4–9]. To date, numerous mutations in *KCNQ1* have been considered responsible for hereditary LQT1, and the type and location of *KCNQ1* mutation are associated with varying clinical severities [10–13]. However, the clinical phenotype of the different mutations and the underlying mechanisms remain poorly understood.

Studies have demonstrated that mutations at the N-terminus of *KCNQ1*, such as Y111C, L114P, and P117L, could affect its transport [14]. Moreover, mutations on the C-loop inactivate the  $I_{Ks}$  mediated by protein kinase A (PKA), causing the inward calcium ion current to increase without confrontation during  $\beta$ -adrenergic stimulation [8]. These studies have provided direct evidence demonstrating that the types of mutation are differently associated with physiological activities and mechanisms; this provides the theoretical basis for drug target screening. However, most experiments have been performed almost exclusively on animal models [15, 16]. Although *KCNQ1*-knockout mice presented with the Jervell and Lange–Nielsen phenotype [17, 18], the mouse heart repolarization  $K^+$  current is a fast, slow-transient outward current, and delayed rectified voltage-gated  $K^+$  current, which cannot reflect the effect of *KCNQ1* deficiency in humans [19]. Hence, the establishment of *KCNQ1*-mutant human embryonic stem cell-derived cardiomyocytes (CMs) is necessary for the mechanistic exploration and drug screening for LQT1 caused by *KCNQ1* mutations.

In recent years, the establishment of disease models and drug screening using human induced pluripotent stem cell-derived CMs (hiPSC-CMs) has become a promising therapeutic approach for cardiovascular diseases [20]. In this study, we developed *KCNQ1*-deficient, *KCNQ1*<sup>L114P/+</sup>, and *KCNQ1*<sup>R190Q/+</sup> human myocardial models using CRISPR/Cas9 system to investigate a well-defined genotype–phenotype correspondence. *KCNQ1*-deficient cells showed serious QT prolongation, irregular rhythm, early post-depolarization (EAD), and  $I_{Kr}$  current insensitivity. *KCNQ1*<sup>L114P/+</sup> CMs showed a significantly longer QT delay than *KCNQ1*<sup>R190Q/+</sup> CMs. Our results showed that MgCl<sub>2</sub>, propranolol, and amiodarone could reverse the abnormal phenotype caused by *KCNQ1* deficiency or mutations separately. The results showed that those models can well reflect the disease phenotype and contribute to the drug screening and accurate treatment of *KCNQ1* mutation-related diseases.

## Methods

### Cell culture and cardiac differentiation of hESC

The hESC line was purchased from Cellapy (Beijing, China) and was routinely maintained in the presence of

PSCeasy medium (Cellapy, China) on six-well plates (Corning, USA) coated with 5% Matrigel (Corning, USA). Medium was changed every day and passaged every 2–3 days with EDTA (Cellapy, China). The cells were grown in a humidified atmosphere of 95% air and 5% CO<sub>2</sub> at 37 °C. The hESCs were differentiated when they reached 70–80% confluence. Medium was changed to the basal differentiation medium. For day 0 to day 2, medium was changed to the basal medium C01 (Cellapy, China). For day 2 to day 4, medium was changed to the basal differentiation medium C02 (Cellapy, China). On day 4, medium was changed to the basal differentiation medium C03 (Cellapy, China) and changed medium every other day. Contracting cells were noted from day 9.

### Genome editing

*KCNQ1* single-stranded guide RNA (sgRNA) (ATGCTA CACGTCGACCGCCA,CAGCCGCCCCAGAGGCC CA,GCTCGAGGAAGTTGTAGACG) was designed using an online tool (<https://www.synthego.com>). We electroporated the epiCRISPR vector and sgRNA (100  $\mu$ l electrotransformation solution (Cellapy, China) plus 2.5  $\mu$ g *KCNQ2* gRNA plasmid) into the cells using the 4D nuclear receptor system and the CA137 programme (Lonza, Germany). The transfected cells were seeded in 6-well plates and cultured overnight in PSCeasy medium 10  $\mu$ M of Rho kinase inhibitor Y-27632. The medium was changed the next day. Drug (puromycin) selection was initiated after 72 h of transfection at a lower concentration of 0.1  $\mu$ g/ml for the first hour and then at 0.3  $\mu$ g/ml until the transfected lines were stable. The surviving cells were collected in 48-well plates and amplified for polymerase chain reaction (PCR) screening. The point mutation cells were prepared by epi-ABEmax/epi-AncBE4max/epi-ABEmax-NG/epi-AncBE4 max-NG plasmid. The plasmid was transfected using Lipofectamine 3000, and then, the transfected cells were selected by blasticidin. The specific methods can refer to the previous research.

### Drug treatment

100 mM 293B, 100  $\mu$ M isoproterenol (ISO), 5  $\mu$ M propranolol, 100  $\mu$ M amiodarone 100  $\mu$ M MgCl<sub>2</sub> (Selleck, USA) were diluted in C05 (Cellapy, China). hESC-CMs were treated with 293B, ISO, Propranolol for 12 h. hESC-CMs were treated with Amiodarone, MgCl<sub>2</sub> for 30 min.

### RNA extraction and RT-PCR

Total RNA from cells was extracted by using TRIZOL Reagent (Invitrogen, USA). An amount of 2  $\mu$ g total RNA was reversed to cDNA by using the GoScript Reverse Transcription System (Promega, USA). Quantitative RT-PCR involved use of SYBR Green II (Takara, Japan) in

the iQ5 system (Bio Rad, Hercules, CA). A comparative CT method was used to analyze the relative changes in gene expression. The results were expressed as relative to the data of GAPDH transcripts (internal control). Primer sequences are listed in Additional file 1: Table S1.

#### Immunofluorescent staining (IF) and imaging analyses

The cells were plated on 20 mm coverslips coated with 5% Matrigel and were fixed with 4% PFA for 15 min. Then, after washing with PBS three times for 5 min, the cells were permeabilized with 0.2% Triton X-100 (Sigma, USA) for 15 min and blocked with 3% BSA (Sigma, USA) for 1 h at room temperature. After that cells were incubated with primary antibodies, overnight at 4 °C. Then, cells were washed by PBS and incubated for 1 h at room temperature in the dark with secondary antibodies (Invitrogen, USA). Cells were washed again as above, mounted with Fluoroshield Mounting Medium with DAPI (4, 6 diamino-2-phenylindole). Images were taken under a Confocal Microscope (Leica DMI 4000B, German). The antibody and their appropriate dilution are provided in Additional file 1: Table S2.

#### Western blot (WB) analysis

Protein from hESC-CMs was extracted by using a Protein Extraction Kit (Promega, USA). The protein concentration of the supernatant was measured by BCA method. The 30 µg protein was separated on 10% SDS-PAGE and transferred to PVDF membrane at 300 mA for 90 min, which was blocked with 5% albumin bovine (BSA) at room temperature for 1 h, then incubated at 4 °C overnight with the primary antibodies, then with IR dye-conjugated secondary antibodies (LI-COR, USA) for 1 h at room temperature. GAPDH was used as an internal control. Blots were exposed and analyzed with use of an Odyssey infrared imaging system (LI-COR Biosciences, USA). The antibody and their appropriate dilution are provided in Additional file 1: Table S2.

#### Flow cytometry

The hESC-CMs under different treatments were singularized with CardioEasy Human Cardiomyocyte Digestive Fluid (Cellapy, China). Observe that most of the clones are detached from the bottom of the plate under the microscope, gently pipette the cells and suck them out, centrifuge, and wash three times with PBS. The cells were stained with different antibodies, filtered through the 300 mesh filter, and immediately analyzed by FACS (Beckman, USA). The cell count is generally 1–2 million. The results were analyzed with Flow Jo X program.

#### Microelectrode array (MEA) analysis

hESC-CMs were digested in CardioEasy Human Cardiomyocyte Digestive Fluid (Cellapy, China), after which  $2 \times 10^4$  cells were plated on a microelectrode array (MEA) pre-coated with 5% Matrigel (Cellapy, China). The next day, 300 µl medium was added to each well. After the hESC-CMs resumed spontaneous beating, the experimental data were recorded on a Maestro EDGE (Axion Biosystems, Inc., Atlanta, USA) according to the MEA manual. Cardiac Analysis Tool, AxIS Navigator, AxIS data export tool, and Origin were used to analyze the data.

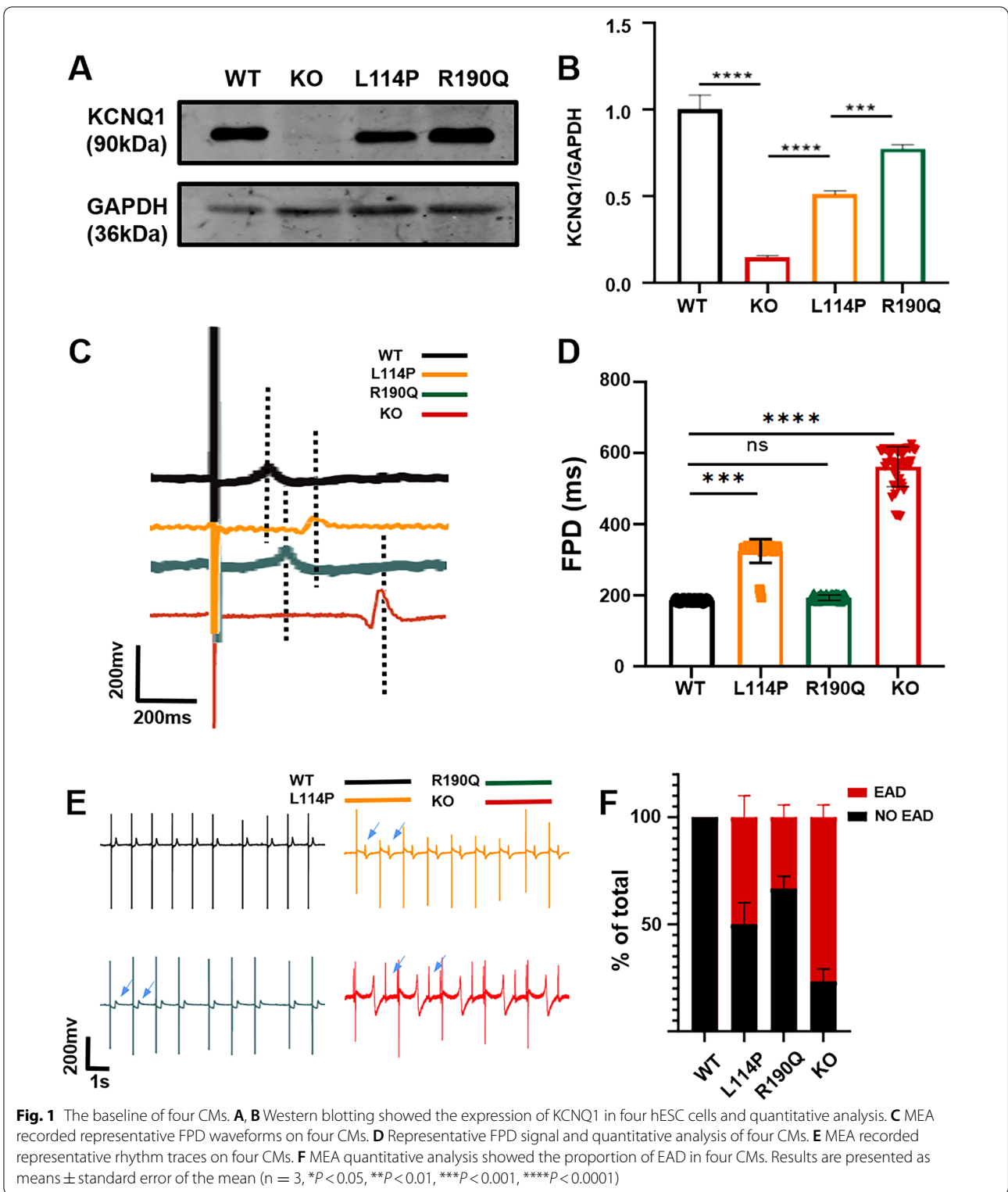
#### Statistical analysis

Results are expressed as mean  $\pm$  SD. Statistical analysis was performed with GraphPad Prism 8.00 for Windows. Two-sided unpaired Student's *t* test was used to compare 2 groups with normal distribution. One-way ANOVA was used to compare 3 or more groups. All tests for normality and homogeneity of variance were passed before *t* test and one-way analysis of variance. *P* values of less than 0.05 were used to denote statistical significance. \**P* < 0.05; \*\**P* < 0.01, \*\*\**P* < 0.001; NS, not significant.

## Results

### Establishment of the *KCNQ1*-knockout and *KCNQ1*-mutant hESC-CM models

We used the CRISPR/Cas9 system to establish a *KCNQ1*-deficient H9 hESC cell model. We designed a highly specific sgRNA targeting *KCNQ1* and electroporated hESC H9 cells with a plasmid containing sgRNA and Cas9 element. Subsequently, the transfected cells were screened using puromycin, and the genotype of the surviving clones was determined using the Sanger sequencing method. Sequencing results revealed that a homozygous clone with a 2-basepair(bp) mutation in *KCNQ1* was obtained (*KCNQ1*<sup>R190Q/+</sup>) (Additional file 2: Fig. S1A). The pluripotency of *KCNQ1*<sup>R190Q/+</sup> was identified using the appropriate markers, and the karyotype and tumorigenic characteristics of stem cells did not change (Fig. S1B–E) *KCNQ1*<sup>R190Q/+</sup> and other hESCs (*KCNQ1*<sup>L114P/+</sup> and *KCNQ1*<sup>-/-</sup>) that were established in our previous work were induced to differentiate into CMs using small molecules with clear chemical compositions (Additional file 3: Fig. S2A) [21]. Immunofluorescence staining of CMs for 30 days showed normal expression of troponin T (TNNT2) and  $\alpha$ -actin (Additional file 3: Fig. S2B). Flow cytometry revealed that the TNNT2 positivity rate of H9 hESC wild type (WT) and *KCNQ1*<sup>-/-</sup> CMs was close to 86% (Additional file 3: Fig. S2C and S2D). We tested the cell viability of the four kinds of hESC-CMs by CCK8, and the results showed that there was no difference in



the cell viability of the four kinds of hESC-CMs (Additional file 3: Fig. S2E). Western blot analysis confirmed the absence of the KCNQ1 protein in  $KCNQ1^{-/-}$  CMs (Fig. 1A, B, Additional file 3: Fig. S2F). Furthermore, the

expression of *KCNQ1* in  $KCNQ1^{L114P/+}$  CMs significantly decreased compared with that in WT and  $KCNQ1^{R190Q/+}$  CMs, suggesting the abnormal *KCNQ1* transport of  $KCNQ1^{L114P/+}$  CMs.

**KCNQ1<sup>-/-</sup>, KCNQ1<sup>L114P/+</sup>, and KCNQ1<sup>R190Q/+</sup> CM models reflect the LQT phenotype**

Differences between KCNQ1<sup>-/-</sup>, KCNQ1<sup>L114P/+</sup>, and KCNQ1<sup>R190Q/+</sup> CMs were observed at the multicellular level using the high-throughput Maestro Edge micro-electrode array (MEA) system [22, 23]. The field potential duration (FPD) was calculated as the time between depolarization and repolarization marked by the beat time and the repolarization peak or T-wave, respectively. FPD can reflect the duration of myocardial QT interval. FPD statistics showed no difference between KCNQ1<sup>R190Q/+</sup> and WT CMs. Moreover, the FPD of KCNQ1<sup>L114P/+</sup> CMs was only slightly prolonged, whereas that of KCNQ1<sup>-/-</sup> CMs was significantly prolonged (Fig. 1C, D). This slight prolongation in KCNQ1<sup>L114P/+</sup> CMs may be due to the lack of repolarization I<sub>Ks</sub> caused by abnormal KCNQ1 transport, which is consistent with the decreased expression of KCNQ1 in KCNQ1<sup>L114P/+</sup> CMs as observed through Western blot analysis. Irregular rhythm and EADs are precursors of ventricular arrhythmias in LQT; therefore, we also used MEA to analyze the rhythm of the three models. The results indicated that KCNQ1<sup>-/-</sup> CMs show obvious arrhythmia and that the proportion of EADs significantly increased compared with WT CMs. KCNQ1<sup>L114P/+</sup> and KCNQ1<sup>R190Q/+</sup> CMs also showed obvious arrhythmia (Fig. 1E, F).

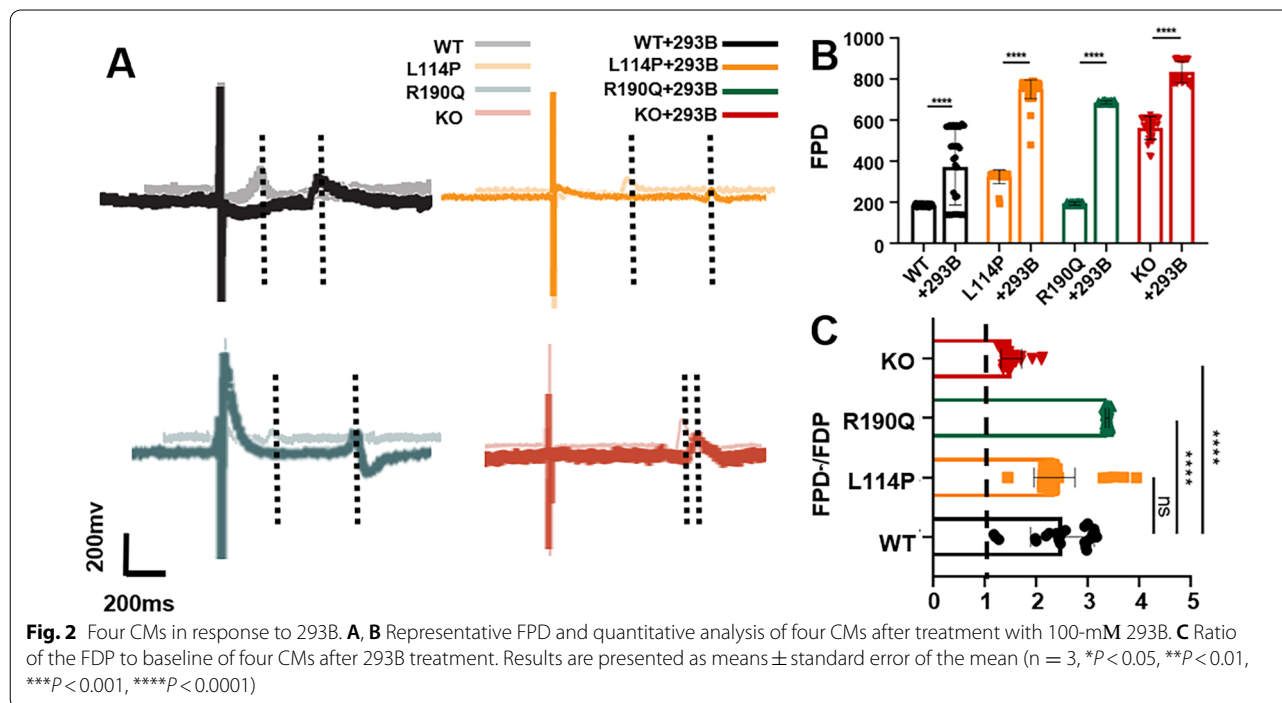
**Response to I<sub>Ks</sub>-specific blocker**

Moreover, we tested the effects of the I<sub>Ks</sub>-specific blocker chromanol 293B on the FPD of the three models [24].

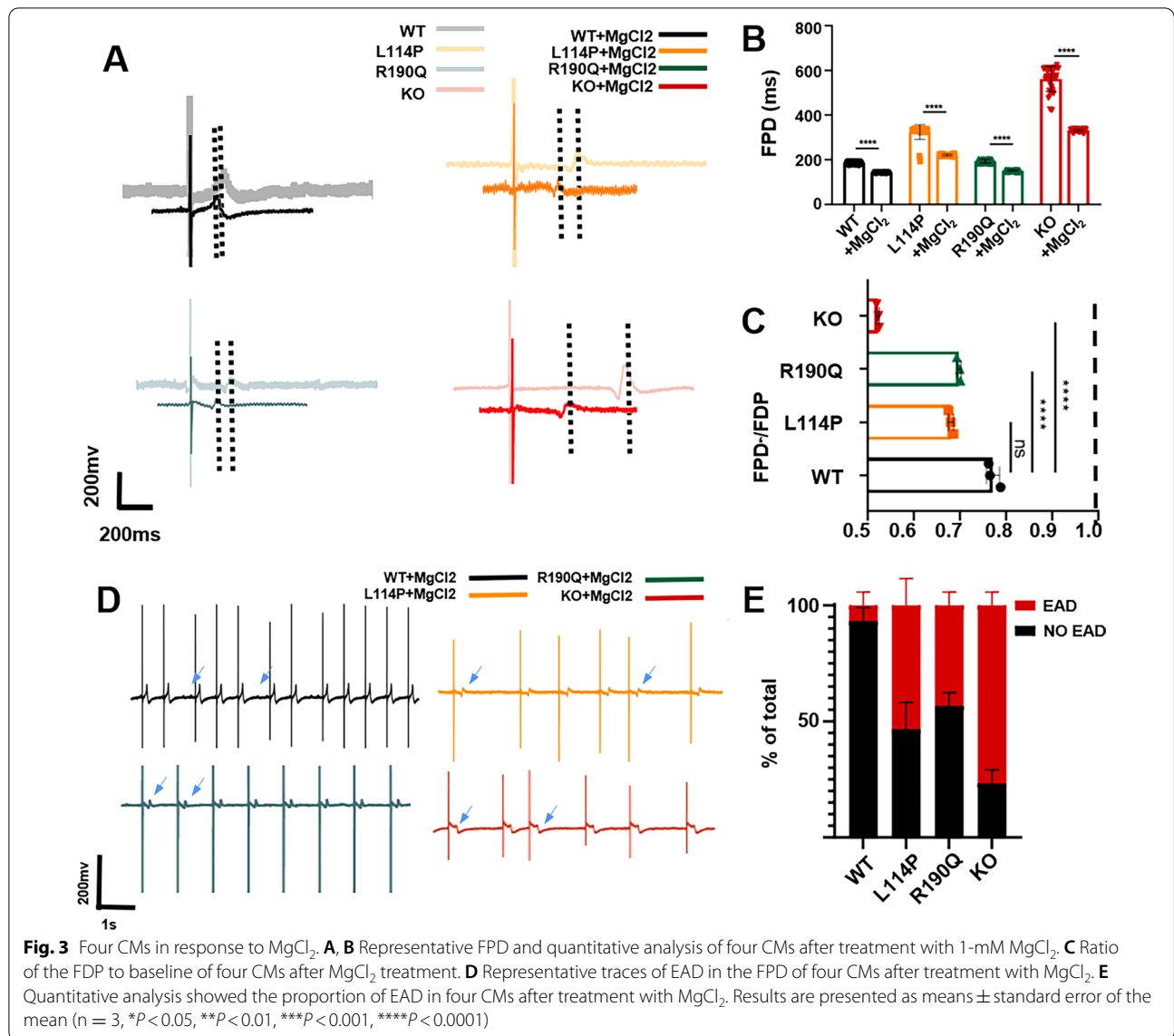
We used the ratio of FPD after dosing to that at baseline (FDP'/FDP) to indicate the extent of FPD change. A value of >1 indicates that the FPD is prolonged, whereas a value of <1 indicates a shortened FPD. Interestingly, the FPD of WT, KCNQ1<sup>L114P/+</sup>, and KCNQ1<sup>R190Q/+</sup> CMs showed prolongation after treatment with 100-mM 293B. In contrast, the FPD of KCNQ1<sup>-/-</sup> CMs did not show significant prolongation as that of KCNQ1<sup>L114P/+</sup> and KCNQ1<sup>R190Q/+</sup> CMs after treatment with 293B (Fig. 2A, B). Meanwhile, the FDP'/FDP of WT, KCNQ1<sup>L114P/+</sup>, and KCNQ1<sup>R190Q/+</sup> CMs was significantly higher than that of KCNQ1<sup>-/-</sup> CMs; however, the FPD prolongation of the knockout CMs is the least obvious (Fig. 2C). These results indicate that the KCNQ1 mutation and knockout models were successfully established.

**Responses to MgCl<sub>2</sub>**

Mg<sup>2+</sup> is the main coenzyme for potassium ion transfer inside and outside a cell. Mg<sup>2+</sup> supplementation can increase potassium ion transport, increase the intracellular potassium concentration, and increase stability of cell membrane and electrocardiogram. Therefore, we observed changes in the FPD of the four CMs after MgCl<sub>2</sub> treatment. MgCl<sub>2</sub> treatment can shorten the FPD of all three models, with the FPD shortening of KCNQ1<sup>-/-</sup> CMs being the most significant (Fig. 3A–C). This suggests that magnesium supplementation is essential for LQT treatment with different mechanisms. However, EAD cannot be eliminated (Fig. 3D, E).



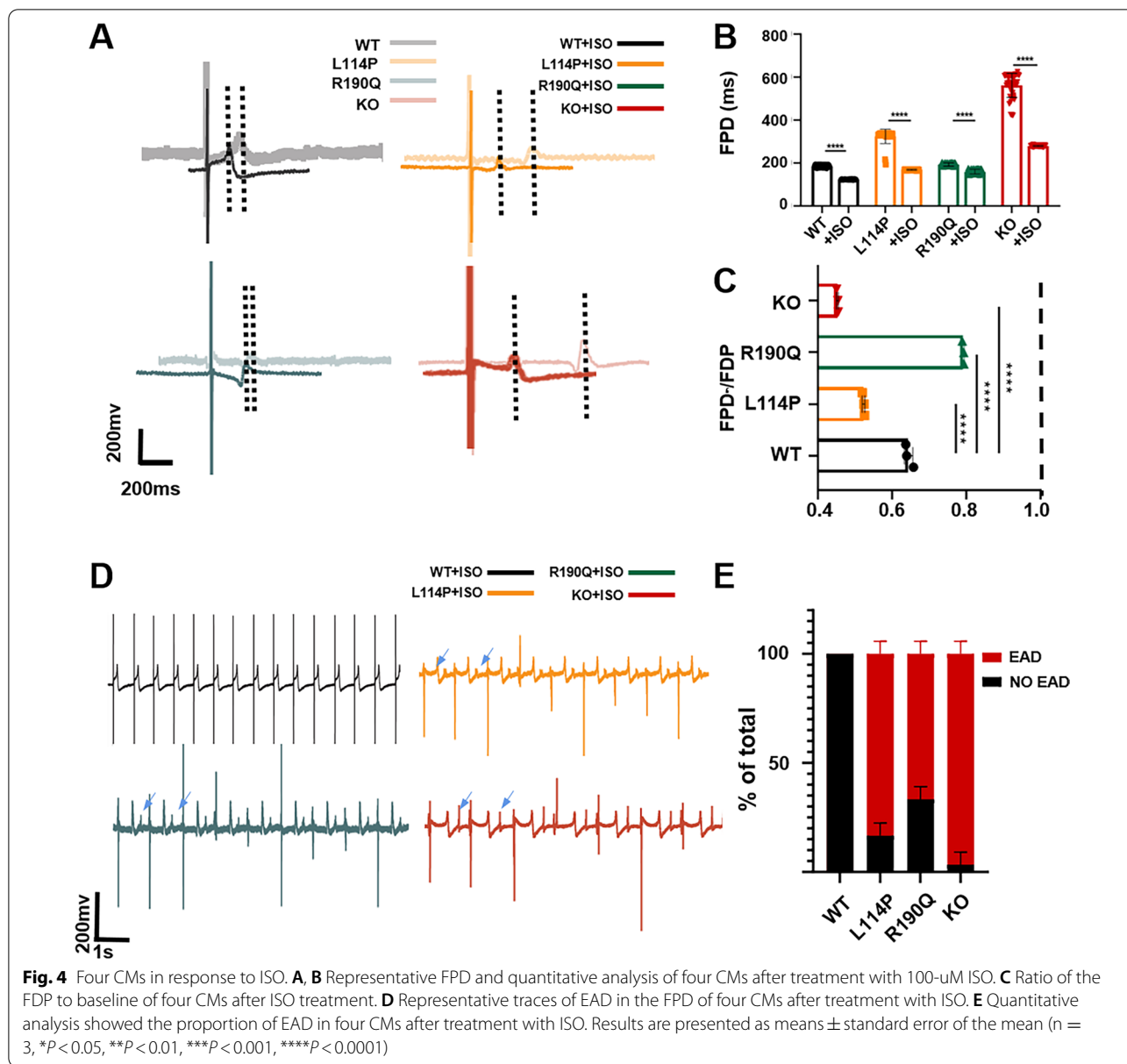




### Responses to isoproterenol

The occurrence of LQT1 is often associated with sympathetic nerve excitement (such as due to exercise or emotional agitation); therefore, sympathetic nerve excitement was simulated using isoproterenol (ISO) treatment [25]. ISO is a β-agonist that binds to β-AR and activates cAMP–PKA-dependent downstream signals, which then promotes the phosphorylation of several target proteins, including the L-type calcium channel and lysine receptor. Subsequently, PKA phosphorylates these proteins and increases the calcium concentration in the sarcoplasm, resulting in the activation of the crossbridge and further enhancement of the contraction of CMs [26]. After treatment with 100-μM ISO, the FPD of WT, KCNQ1<sup>L114P/+</sup>, and KCNQ1<sup>-/-</sup> CMs was significantly shortened

compared with the baseline (Fig. 4A–C). This phenotypic change was caused by the agonistic effect of ISO. However, the FPD of KCNQ1<sup>R190Q/+</sup> CMs did not appear to be significantly shortened, suggesting that KCNQ1<sup>R190Q/+</sup> CMs are not sensitive to ISO. This is consistent with the results of previous studies demonstrating that mutations in the C-loop, such as those in KCNQ1<sup>R190Q/+</sup> CMs, may indeed inactivate Kv7.1’s response to PKA stimulation [12]. Furthermore, WT CMs did not show arrhythmia after ISO treatment, whereas KCNQ1<sup>L114P/+</sup> CMs and KCNQ1<sup>R190Q/+</sup> CMs both showed arrhythmia aggravation (Fig. 4D, E). Both point mutation cells showed the arrhythmia phenotype under β-adrenergic stimulation, which was consistent with the phenotype where LQT1 was more easily induced under sympathetic



excitation; this indicates that the point mutation model can reflect the response of the myocardium to sympathetic excitation.

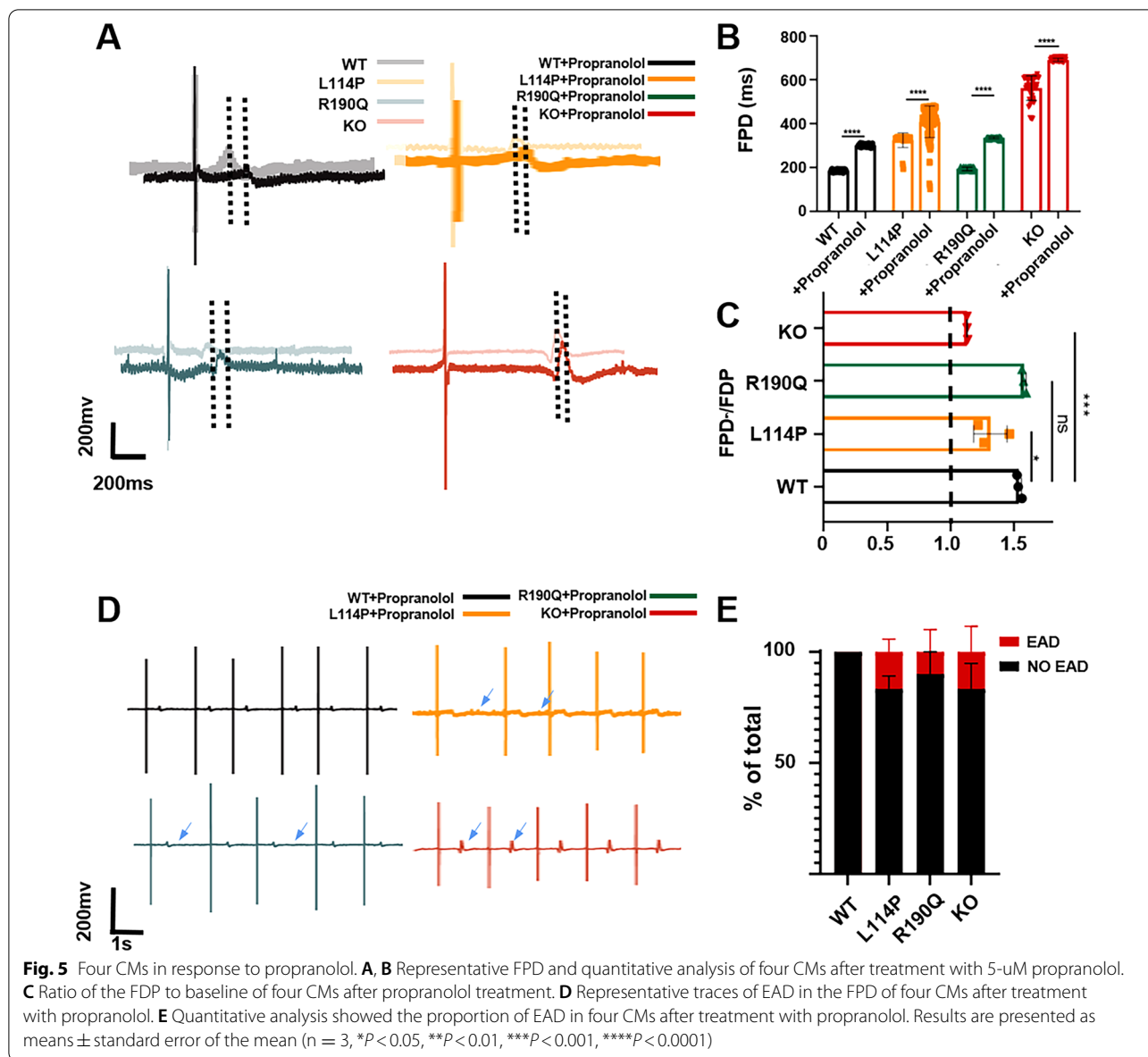
**Responses to propranolol**

$\beta$ -blockers can directly decrease  $\beta$ -adrenergic signaling and show antiarrhythmic effects [26]. Propranolol, a  $\beta$ -blocker, is one of the most common drugs used in the clinical treatment of LQT. Therefore, we subjected the CM models to this drug and examined the responses. The results showed that the three CM models showed prolongation of the FPD (Fig. 5A–C). Moreover, the slowing of the heart rhythm and arrhythmia in  $KCNQ1^{-/-}$ ,  $KCNQ1^{L114P/+}$ , and  $KCNQ1^{R190Q/+}$  CMs was significantly

decreased compared with the baseline values (Fig. 5D, E). Propranolol can improve the arrhythmia phenotype of the three  $KCNQ1$ -mutant myocardial models, including  $KCNQ1^{-/-}$  CMs, indicating that propranolol has therapeutic effects on LQT1 through multiple mechanisms.

**Responses to amiodarone**

We also tested the response of the three models to other common LQT medications used clinically. Amiodarone is a type III multi-ion channel blocker that can selectively prolong the repolarization time of the myocardium and is suitable for various ventricular arrhythmias [27]. After treatment with 100- $\mu$ M amiodarone, WT,  $KCNQ1^{L114P/+}$ ,  $KCNQ1^{R190Q/+}$ , and  $KCNQ1^{-/-}$  CMs showed significant



FPD prolongation; however, *KCNQ1*<sup>-/-</sup> CMs had the smallest FPD extension (Fig. 6A–C). Amiodarone alleviated the arrhythmia phenotype of *KCNQ1*<sup>L114P/+</sup> CMs but weakened the pulsation of *KCNQ1*<sup>-/-</sup> CMs (Fig. 6D, E). These results suggest that amiodarone has a good therapeutic effect on LQT1 with different mutations; however, it is not suitable for treating patients with *KCNQ1* large fragment deletion.

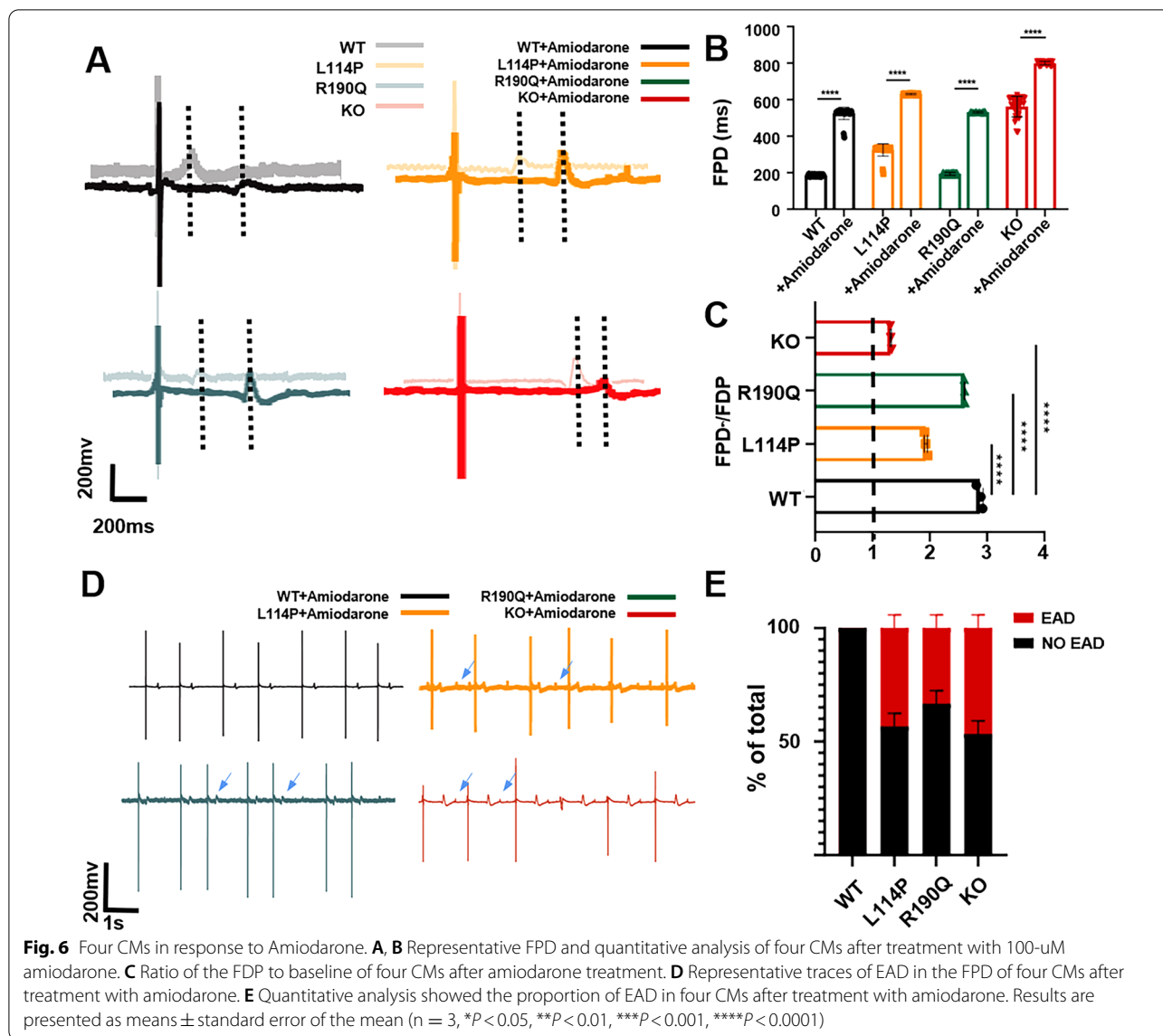
**Discussion**

*KCNQ1* mutation is strongly correlated with LQT1. In this study, we used MEA to investigate the response of different genotypes of *KCNQ1* mutations to different

drugs to determine the underlying mechanisms of different *KCNQ1* mutations. Our results indicated that *KCNQ1*-deficient and *KCNQ1*-mutant cells showed varying serious QT prolongation and irregular rhythm and that these can be corrected using *I*<sub>Ks</sub>-specific,  $\beta$ , and multi-ion channel blockers. These results suggest that the novel hiPSC-CM models are helpful tools in the determination of pathogenic mechanisms and drug screening for LQT1 induced by *KCNQ1* mutations.

Congenital LQTS is a life-threatening arrhythmic syndrome and is the leading cause of sudden death among young people [28]. The typical characteristics of LQTS are prolongation of the QT interval on electrocardiography and the presence of syncope or cardiac





arrest mainly due to emotional or physical stress. The three main genotypes of LQTS—LQT1, LQT2, and LQT3—account for 80–90% of all 15 gene mutations found in patients with LQTS [14]. As the main genetic genotype of LQT, LQT1 is caused by mutations in the slow potassium ( $K^+$  outward current channel encoded by *KCNQ1* [29]). *KCNQ1* encodes the  $\alpha$ -subunit of the  $K^+$  channel  $Kv7.1$ , producing a depolarized  $I_{Ks}$  current that increases through sympathetic activation and is critical for QT adaptation as the heart rate increases [30]. When  $I_{Ks}$  is defective, the QT interval cannot be appropriately shortened during tachycardia, resulting in high-grade arrhythmia. Homozygous mutations or compound heterozygous mutations in *KCNQ1* can lead to Jervell and Lange-Nielsen syndrome, which is

characterized by decreased inner ear  $I_{Ks}$  and deafness [31]. There are more than 100 pathogenic heterozygous mutations in *KCNQ1*, each with a different effect on the polymeric  $K^+$  channel. Mutant and WT protein subunits may assemble together and have a significant negative effect on the current. Alternatively, certain mutant subunits may fail to co-assemble with the WT peptide, resulting in the loss of function that reduces  $I_{Ks}$  by  $\leq 50\%$  (haploinsufficiency). The latter may also be due to mutations interfering with intracellular subunit transport, preventing the mutant peptide from reaching the cell membrane.

The complex mutation mechanism increases the difficulty of providing precise treatment for LQT1; therefore, establishing an effective model is essential to

enable mechanism exploration and drug screening. Due to the huge difference in the cardiac functions of mice and humans,  $I_{Ks}$  does not participate in repolarization in mice, making it difficult to use mice models. hiPSC-CMs can simulate human cardiac action potential, which is a good application prospect in disease modeling. Models constructed using patient-derived hiPSC-CMs have been shown to be effective [32]. However, patient-derived hiPSC-CMs cannot accurately reflect the gene–phenotype relationship due to the influence of background genes. Moreover, obtaining patient-derived cardiac muscles is difficult. Therefore, the use of gene editing to artificially prepare myocardium with point mutation for disease simulation has good application prospects. In previous studies, our research group constructed  $KCNQ1^{L114P/+}$  and  $KCNQ1^{R190Q/+}$  models using BaseEditor's method.

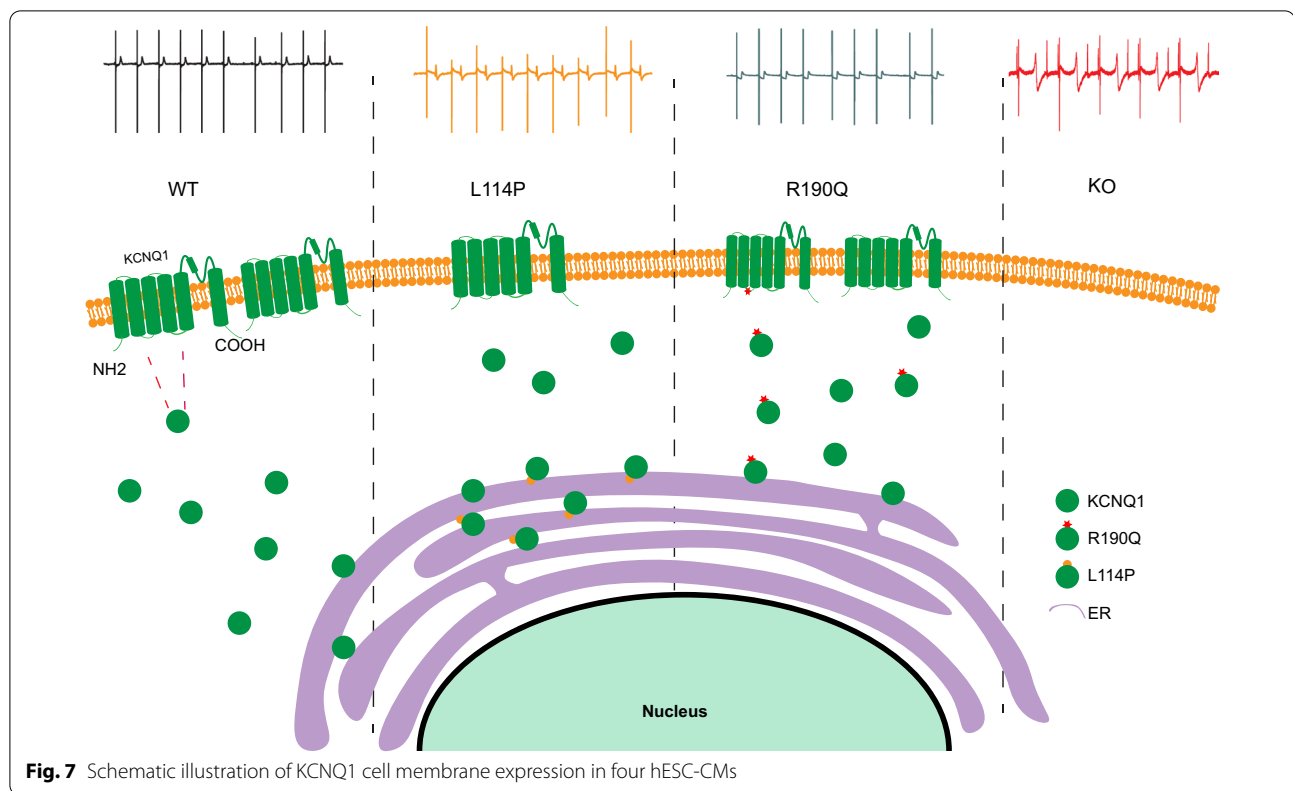
$KCNQ1^{L114P/+}$  and  $KCNQ1^{R190Q/+}$  are serious pathogenic mutations in the LQT1 phenotypes. The pathogenic mechanism of LQT1 caused by  $KCNQ1$  mutation mainly includes the following categories: defects in ion permeation, channel gating, trafficking defect,  $KCNQ1$ – $KCNE1$  interaction, PKA-mediated signaling pathway, PIP2 binding, and calmodulin binding [33].  $KCNQ1^{L114P/+}$  is a mutation at the N-terminus of  $KCNQ1$  that affects the upper membrane transport of  $KCNQ1$  [21], whereas  $KCNQ1^{R190Q/+}$  is a mutation located on the C-ring of  $KCNQ1$ . Studies have proven that such mutations may reduce the sensitivity of  $KCNQ1$  to PKA, leading to the inability of  $I_{Ks}$  to significantly increase when stimulated by adrenaline, thus inducing arrhythmias. The electrophysiological phenotypes of the two models were preliminarily detected and found to be able to reflect the disease phenotypes. Furthermore, due to the diverse pathogenic mechanisms of  $KCNQ1$ , there is no effective human  $KCNQ1$  deletion model to clarify the direct phenotype of  $KCNQ1$ . Large fragment  $KCNQ1$  deletion cases have been reported, and the development of a  $KCNQ1$  deletion model helps improve the treatment of this disease. Even though  $KCNQ1$ -knockout mice were present and seen to exhibit the Jervell and Lange–Nielsen syndrome, the QT prolongation phenotype was thought to be mediated by extracardial factors because  $I_{Ks}$  did not participate in the mouse repolarization process [12]. Therefore, we developed an hESC-CM model without  $KCNQ1$ .

In this study, the MEA results showed that the FPD of  $KCNQ1^{-/-}$  CMs was significantly prolonged compared with that of WT CMs, indicating that the absence of  $I_{Ks}$  prolonged the repolarization time course of CMs. The FPD of  $KCNQ1^{L114P/+}$  CMs was prolonged, whereas that of  $KCNQ1^{R190Q/+}$  CMs was not different from that of WT CMs. This suggests that the L114P mutation decreases the upper membrane of  $KCNQ1$ , whereas

R190Q does not cause QT prolongation at baseline. Furthermore,  $KCNQ1^{-/-}$  CMs showed arrhythmias even at baseline, suggesting that the complete loss of  $I_{Ks}$  has a severe effect on myocardial action potentials. When treated with 293B, the FPD of  $KCNQ1^{-/-}$  CMs was not significantly prolonged, whereas that of  $KCNQ1^{L114P/+}$  and  $KCNQ1^{R190Q/+}$  CMs was, indicating that this insensitivity was due to the deletion of Kv7.1 channel encoded by  $KCNQ1$ . The baseline phenotype initially reflected the success of model construction and the phenotype of the disease. A schematic of the mechanism can be seen in Fig. 7.

LQT1 often occurs during exercise and emotional arousal; therefore, we used ISO to simulate sympathetic excitation. After ISO treatment, WT,  $KCNQ1^{-/-}$ , and  $KCNQ1^{L114P/+}$  CMs showed significant shortening of the FPD, indicating that they responded to ISO's excitement. However,  $KCNQ1^{R190Q/+}$  CMs showed insensitivity to ISO stimulation, confirming that this mutation indeed causes the passivation of Kv7.1 channel to PKA stimulation. Under ISO stimulation, all models showed aggravation of the arrhythmia phenotype, partially simulated LQT1 caused by  $KCNQ1$  mutation under sympathetic excitation. Subsequently, we used common clinical LQT drug treatments to explore the response of different mutations to different drugs. The use of propranolol significantly prolonged the FPD of the three types of CMs and maintained cardiac rhythm stability in  $KCNQ1^{-/-}$ ,  $KCNQ1^{L114P/+}$ , and  $KCNQ1^{R190Q/+}$  CMs, indicating that  $\beta$ -blockers have good therapeutic effects on LQT with different mechanisms. Amiodarone has a greater prolongation effect on the FPD in the three models; however, amiodarone treatment may result in reduced pulsation of  $KCNQ1^{-/-}$  CMs, suggesting that it is not suitable for treating patients with large fragment  $KCNQ1$  deletion.  $MgCl_2$  treatment can reduce the FPD of the three models and has a good effect on heart rhythm stability; this reflects the importance of magnesium supplementation for patients under treatment for LQT.

This study established a hESC-CM model of  $KCNQ1$  deletion, clarified the relationship between the genotype and phenotype of  $KCNQ1$ , and bridged the gap in terms of a human model of  $KCNQ1$  deletion. Moreover,  $KCNQ1^{-/-}$ ,  $KCNQ1^{L114P/+}$ , and  $KCNQ1^{R190Q/+}$  CMs showed different responses to different drug interventions, and their phenotypic changes were consistent with the mechanisms proposed in previous studies, indicating that the artificial absence and pitting myocardial model can reflect the LQT phenotype. As a good disease model, it shows great potential for application in precision treatment and drug screening. However, because the phenotype of hESC-CMs is closer to immature myocardium, there are some differences



between hESC-CMs and adult myocardium in electrophysiological phenotype. This difference makes the hESC-CMs model unable to fully simulate the pathological phenotype and drug response of human myocardium. At the same time, we use the 2D myocardial differentiation method in this study, and the complete heart structure is not constructed, which may also lead to the difference between the drug response of this model and that under normal physiological conditions. These problems limit the application of the model in the clinical field. In the follow-up study, we will consider constructing engineered myocardial tissue (EHT) model to better approach the physiological phenotype.

### Conclusion

In this study, we developed a *KCNQ1* defect model using the CRISPR/Cas9 system. Simultaneous electrophysiological detection was performed on *KCNQ1*<sup>-/-</sup>, *KCNQ1*<sup>L114P/+</sup>, and *KCNQ1*<sup>R190Q/+</sup> CMs. The *KCNQ1*<sup>-/-</sup> CM model showed significant QT interval prolongation, arrhythmia, and sensitivity to other ion channel blockers. This model can be used as an important tool to improve our understanding of the basic pathological mechanism of *KCNQ1* dysfunction, define the genotype–phenotype correspondence, and promote

drug development. Furthermore, under different intervention conditions, the phenotypes of *KCNQ1*<sup>L114P/+</sup> and *KCNQ1*<sup>R190Q/+</sup> CMs showed different responses, suggesting that 114 and 190 have different pathogenic mechanisms. It provides an effective model for studying the different pathogenic mechanisms of LQT and confirms the feasibility of preparing a single-gene genetic disease model through gene editing.

### Abbreviations

IKs: Delayed-rectifier potassium current; hESC: Human embryonic stem cell; LQTS: Long-QT syndrome; MEA: Microelectrode array; CM: Cardiomyocyte; hiPSC-CMs: Human induced pluripotent stem cell-derived CMs; EAD: Early post-depolarization; sgRNA: Single-stranded guide RNA; ISO: Isoproterenol; FPD: Field potential duration; WT: Wild type.

### Supplementary Information

The online version contains supplementary material available at <https://doi.org/10.1186/s13287-022-02964-3>.

**Additional file 1.** Supplementary Figure legends.

**Additional file 2. Supplemental Figure 1.** *KCNQ1* point mutation did not affect the pluripotency nature of hESC.

**Additional file 3. Supplemental Figure 2.** *KCNQ1* knockout and point mutations(L114P、R190Q) did not affect the ability of cardiac differentiation.

### Acknowledgements

The authors thank the Cellapy Biological Technology Company (Beijing, CHN) for providing technical support for the hESC-CMs experiments.

### Author contributions

MC, FL, YXS, TWG, YXJ, and WJL conceived the idea and designed the project. YXS, TWG, and YXJ performed most of the experiments and analyzed the data. HYW, MZ, MQ, and MQJ provided technical assistance. YXS, TWG, and YXJ wrote and revised the paper. All authors read and approved the final manuscript.

### Funding

This project has been supported by the National Natural Science Foundation of China (Grant Nos. 81970205, 82070272).

### Availability of data and materials

All data generated or analyzed during this study are included in this published article.

### Declarations

#### Ethics approval and consent to participate

Not applicable.

#### Consent for publication

Not applicable.

#### Competing interests

The authors declare that they have no conflict of interest.

### Author details

<sup>1</sup>Department of Cardiology, Peking University Third Hospital, 49 Huayuan North Road, Haidian District, Beijing 100191, China. <sup>2</sup>Beijing Lab for Cardiovascular Precision Medicine, Anzhen Hospital, Capital Medical University, Beijing 100029, China. <sup>3</sup>State Key Laboratory of Cardiovascular Disease, Fuwai Hospital, National Center for Cardiovascular Diseases, Chinese Academy of Medical Sciences and Peking Union Medical College, Beijing 100037, China. <sup>4</sup>Shenzhen Key Laboratory of Cardiovascular Disease, Fuwai Hospital Chinese Academy of Medical Sciences, Chinese Academy of Medical Sciences and Peking Union Medical College, Shenzhen 518057, China. <sup>5</sup>Department of Cell Biology, School of Basic Medical Sciences, Peking University Health Science Center, Beijing 100191, China. <sup>6</sup>Department of Cardiology, The Second Affiliated Hospital of Zhengzhou University, Jingba Road, Zhengzhou 450053, China.

Received: 11 January 2022 Accepted: 20 March 2022

Published online: 28 June 2022

### References

- Schwartz PJ, Ackerman MJ, Antzelevitch C, Bezzina CR, Borggrefe M, Cuneo BF, et al. Inherited cardiac arrhythmias. *Nat Rev Dis Primers*. 2020;6(1):58.
- Schwartz PJ, Stramba-Badiale M, Crotti L, Pedrazzini M, Besana A, Bosi G, et al. Prevalence of the congenital long-QT syndrome. *Circulation*. 2009;120(18):1761–7.
- Schwartz PJ, Crotti L, Insolia R. Long-QT syndrome: from genetics to management. *Circ Arrhythm Electrophysiol*. 2012;5(4):868–77.
- Wang Q, Curran ME, Splawski I, Burn TC, Millholland JM, VanRaay TJ, et al. Positional cloning of a novel potassium channel gene: KVLQT1 mutations cause cardiac arrhythmias. *Nat Genet*. 1996;12(1):17–23.
- Crotti L, Odening KE, Sanguinetti MC. Heritable arrhythmias associated with abnormal function of cardiac potassium channels. *Cardiovasc Res*. 2020;116(9):1542–56.
- Barhanin J, Lesage F, Guillemare E, Fink M, Lazdunski M, Romey G. K(V) LQT1 and IsK (minK) proteins associate to form the I(Ks) cardiac potassium current. *Nature*. 1996;384(6604):78–80.
- Sanguinetti MC, Curran ME, Zou A, Shen J, Spector PS, Atkinson DL, et al. Coassembly of K(V)LQT1 and minK (IsK) proteins to form cardiac I(Ks) potassium channel. *Nature*. 1996;384(6604):80–3.
- Catterall WA. Ion channel voltage sensors: structure, function, and pathophysiology. *Neuron*. 2010;67(6):915–28.
- Sun J, MacKinnon R. Cryo-EM structure of a KCNQ1/CaM complex reveals insights into congenital long QT syndrome. *Cell*. 2017;169(6):1042–50 e9.
- Moss AJ, Shimizu W, Wilde AA, Towbin JA, Zareba W, Robinson JL, et al. Clinical aspects of type-1 long-QT syndrome by location, coding type, and biophysical function of mutations involving the KCNQ1 gene. *Circulation*. 2007;115(19):2481–9.
- Kapa S, Tester DJ, Salisbury BA, Harris-Kerr C, Punliya MS, Alders M, et al. Genetic testing for long-QT syndrome: distinguishing pathogenic mutations from benign variants. *Circulation*. 2009;120(18):1752–60.
- Barsheshet A, Goldenberg I, O-Uchi J, Moss AJ, Jons C, Shimizu W, et al. Mutations in cytoplasmic loops of the KCNQ1 channel and the risk of life-threatening events: implications for mutation-specific response to beta-blocker therapy in type 1 long-QT syndrome. *Circulation*. 2012;125(16):1988–96.
- Schwartz PJ, Moreno C, Kotta MC, Pedrazzini M, Crotti L, Dagradi F, et al. Mutation location and IKs regulation in the arrhythmic risk of long QT syndrome type 1: the importance of the KCNQ1 S6 region. *Eur Heart J*. 2021;42(46):4743–55.
- Dahimene S, Alcolea S, Naud P, Jourdon P, Escande D, Brasseur R, et al. The N-terminal juxtamembranous domain of KCNQ1 is critical for channel surface expression: implications in the Romano-Ward LQT1 syndrome. *Circ Res*. 2006;99(10):1076–83.
- Casimiro MC, Knollmann BC, Ebert SN, Vary JC Jr, Greene AE, Franz MR, et al. Targeted disruption of the Kcnq1 gene produces a mouse model of Jervell and Lange-Nielsen Syndrome. *Proc Natl Acad Sci USA*. 2001;98(5):2526–31.
- Casimiro MC, Knollmann BC, Yamoah EN, Nie L, Vary JC Jr, Sirenko SG, et al. Targeted point mutagenesis of mouse Kcnq1: phenotypic analysis of mice with point mutations that cause Romano-Ward syndrome in humans. *Genomics*. 2004;84(3):555–64.
- Ergul Y, Kafali HC, Cilsal E, Yukcu B, Yaman I, Cetinkaya Isik F, et al. Prevalence of Jervell–Lange Nielsen syndrome in children with congenital bilateral sensorineural hearing loss. *Turk Kardiyol Dern Ars*. 2021;49(5):368–76.
- Torrado R, Fernandez G, Ganoza CA, Maneiro E, Garcia D, Sonicheva-Paterson N, et al. A cryptic splice-altering KCNQ1 variant in trans with R259L leading to Jervell and Lange-Nielsen syndrome. *NPJ Genom Med*. 2021;6(1):21.
- Tosaka T, Casimiro MC, Rong Q, Tella S, Oh M, Katchman AN, et al. Nicotine induces a long QT phenotype in Kcnq1-deficient mouse hearts. *J Pharmacol Exp Ther*. 2003;306(3):980–7.
- Wang Y, Liang P, Lan F, Wu H, Lisowski L, Gu M, et al. Genome editing of isogenic human induced pluripotent stem cells recapitulates long QT phenotype for drug testing. *J Am Coll Cardiol*. 2014;64(5):451–9.
- Qi T, Wu F, Xie Y, Gao S, Li M, Pu J, et al. Base editing mediated generation of point mutations into human pluripotent stem cells for modeling disease. *Front Cell Dev Biol*. 2020;8:590581.
- Clements M, Thomas N. High-throughput multi-parameter profiling of electrophysiological drug effects in human embryonic stem cell derived cardiomyocytes using multi-electrode arrays. *Toxicol Sci*. 2014;140(2):445–61.
- Ban K, Wile B, Cho KW, Kim S, Song MK, Kim SY, et al. Non-genetic purification of ventricular cardiomyocytes from differentiating embryonic stem cells through molecular beacons targeting IRX-4. *Stem Cell Rep*. 2015;5(6):1239–49.
- Lerche C, Bruhova I, Lerche H, Steinmeyer K, Wei AD, Strutz-Seebohm N, et al. Chromanol 293B binding in KCNQ1 (Kv7.1) channels involves electrostatic interactions with a potassium ion in the selectivity filter. *Mol Pharmacol*. 2007;71(6):1503–11.
- Swan H, Viitasalo M, Piippo K, Laitinen P, Kontula K, Toivonen L. Sinus node function and ventricular repolarization during exercise stress test in long QT syndrome patients with KvLQT1 and HERG potassium channel defects. *J Am Coll Cardiol*. 1999;34(3):823–9.
- Johnson DM, Antoons G. Arrhythmogenic mechanisms in heart failure: linking beta-adrenergic stimulation, stretch, and calcium. *Front Physiol*. 2018;9:1453.

27. Martino E, Bartalena L, Bogazzi F, Braverman LE. The effects of amiodarone on the thyroid. *Endocr Rev.* 2001;22(2):240–54.
28. Steinberg C. Diagnosis and clinical management of long-QT syndrome. *Curr Opin Cardiol.* 2018;33(1):31–41.
29. Retraction of: Systematic evaluation of KCNQ1 variant using ACMG/AMP guidelines and risk stratification in long QT syndrome type 1. *Circ Genom Precis Med.* 2021;14(2):e000079.
30. Swartz KJ. Sensing voltage across lipid membranes. *Nature.* 2008;456(7224):891–7.
31. Schwartz PJ, Spazzolini C, Crotti L, Bathen J, Amlie JP, Timothy K, et al. The Jervell and Lange-Nielsen syndrome: natural history, molecular basis, and clinical outcome. *Circulation.* 2006;113(6):783–90.
32. Itzhaki I, Maizels L, Huber I, Zwi-Dantsis L, Caspi O, Winterstern A, et al. Modelling the long QT syndrome with induced pluripotent stem cells. *Nature.* 2011;471(7337):225–9.
33. Bohnen MS, Peng G, Robey SH, Terrenoire C, Iyer V, Sampson KJ, et al. Molecular pathophysiology of congenital long QT syndrome. *Physiol Rev.* 2017;97(1):89–134.

### Publisher's Note

Springer Nature remains neutral with regard to jurisdictional claims in published maps and institutional affiliations.

Ready to submit your research? Choose BMC and benefit from:

- fast, convenient online submission
- thorough peer review by experienced researchers in your field
- rapid publication on acceptance
- support for research data, including large and complex data types
- gold Open Access which fosters wider collaboration and increased citations
- maximum visibility for your research: over 100M website views per year

At BMC, research is always in progress.

Learn more [biomedcentral.com/submissions](https://biomedcentral.com/submissions)

